Front. Chem. Sci. Eng. 2023, 17(7): 976–989
https://doi.org/10.1007/s11705-022-2237-0

RESEARCH ARTICLE

Protective effects of lignin fractions obtained from grape seeds against bisphenol AF neurotoxicity via antioxidative effects mediated by the Nrf2 pathway

Bowen Yan[1*], Geng Lu[3*], Rong Wang[4*], Shixiong Kang[2], Caoxing Huang[1], Hao Wu (✉)[2], Qiang Yong (✉)[1]

1 Jiangsu Co-Innovation Center of Efficient Processing and Utilization of Forest Resources, College of Chemical Engineering, Nanjing Forestry University, Nanjing 210037, China
2 Department of Biomedical Engineering, School of Biomedical Engineering and Informatics, Nanjing Medical University, Nanjing 211166, China
3 Department of Emergency, Nanjing Drum Tower Hospital, The Affiliated Hospital of Nanjing University Medical School, Nanjing 210008, China
4 State Key Laboratory of Analytical Chemistry for Life Science & Jiangsu Key Laboratory of Molecular Medicine, Medical School, Nanjing University, Nanjing 210093, China

Abstract Lignin exhibits antioxidative and various other biological properties. However, its neuroprotection capability has rarely been studied. In this study, three types of lignin with different structures were prepared from grape seeds by using different isolation techniques. The antioxidative and neuroprotective effects of the lignin fractions were evaluated with the apoptosis model of murine neuroectodermal (NE-4C) neural stem cells stimulated with bisphenol AF. The results demonstrated that the half maximal inhibitory concentration for scavenging 2,2-diphenyl-1-picrylhydrazyl with water-soluble lignin (L-W, 58.19 μg·mL^{-1}) was lower than those of lignin in the autohydrolyzed residue of grape seeds (84.27 μg·mL^{-1}) and original lignin in grape seeds (99.44 μg·mL^{-1}). BPAF exposure had negative effects on the reactive oxygen species, malondialdehyde content, and superoxide dismutase and glutathione peroxidase activities in NE-4C cells, which can be reversed by using the prepared lignin to reduce oxidative stress. An immunofluorescence assay demonstrated that grape seed lignin induced protective effects on BPAF-injured NE-4C cells via the nuclear factor erythroid 2-related Factor 2 pathway. In addition, correlational analyses showed that lignin (L-W) with lower molecular weights and noncondensed phenolic hydroxyl group content and higher contents of COOH groups effectively prevented cell apoptosis, scavenged reactive oxygen species, and ensured protection from nerve injury. This study demonstrated that grape seed lignin can be used as a neuroprotective agent and serves as a demonstration of active lignin production from grape seed waste.

Keywords grape seed lignin, structure, antioxidant, NE-4C cells, neuroprotection

1 Introduction

Lignin is a three-dimensional polyaromatic biopolymer and a rich renewable resource in biomass. Approximately 45 million tons of kraft lignin is produced annually worldwide [1]. Lignin is a phenolic polymer commonly found in the cell walls of different plants and biomasses. The natural amorphous structure of lignin is determined by its widespread branching, which primarily comprises three types of 4-hydroxyphenylpropane structures, *p*-hydroxyphenyl (*H*), guaiacyl (*G*), and syringyl (*S*) [2]. Recently, lignin has been identified as a unique bioactive natural high-molecular-weight polymer that has antioxidant, antibacterial, and UV resistance properties due to its different functional groups (hydroxyl and carboxyl groups) [3–5]. Lignin is covalently linked with different polysaccharides in the cell wall. The complicated linkages with different components in the cell wall make it difficult to separate lignin and extract it from cell walls. Hence, different technologies using solvents should be used to obtain lignin from the cell walls of biomass.

Received July 4, 2022; accepted August 18, 2022

E-mails: wuhao_njmu@outlook.com (Wu H.),
swhx@njfu.edu.cn (Yong Q.)

* These authors contributed equally to this work.

Various solvents, such as water, acid solution, alkali solution, and organic solvents, have been proposed for isolating different lignin fractions from biomass and plants [6]. Although the various extraction procedures yield distinct forms of lignin, using the same extraction method with different process parameters can affect the structure and properties of lignin [7]. Extraction of lignin from milled wood lignin with organic solvents is the most commonly used method. The obtained milled wood lignin is considered the classical lignin present in the cell walls of biomass. In addition, the low molecular weight (M_w) of water-soluble lignin (L-W) in autohydrolysate has been used to prepare the lignin fraction because it has a higher content of functional groups than lignin obtained via organic solvent extraction [8,9]. Lignin prepared using these methods has been used to study its biological activity in different biofields.

The strength of the antioxidant activity of lignin is determined by its heterogeneity and diversity, which are regulated by different extraction and isolation processes [10]. Additionally, the different molecular weights and functional groups of lignin can confer different biological capabilities. For instance, the higher amounts of *S* and *G* phenylpropane groups, ample phenolic hydroxyl groups, and lower molecular weight of lignin endow it with a greater ability to scavenge free radicals and reactive oxygen species (ROS), which are positively correlated with its oxidant resistance [10–13]. In addition to antioxidant, antibacterial, and antiultraviolet properties, lignin also possesses anti-inflammatory [14] and neuroprotective properties [15–17]. By blocking the NF-κB, MAPK, TRAF6-NF-κB, and Jak2-Stat3 signaling pathways, lignin and its derivatives can reduce the damage caused by microglia-mediated neuroinflammation and protect against cerebral ischemia-reperfusion injury [15–17]. It is well known that bisphenol A (BPA) is an environmental endocrine disruptor with neurotoxicity. Structural analogs of BPA, including bisphenol AF (BPAF), bisphenol F and bisphenol S, have been widely used in industry in recent years. In addition, BPAF is also used in food packaging, and its harm is widespread. It has been reported that BPA and its structural analogs can cause oxidative stress in the nervous systems of zebrafish and interfere with transcription of nervous system genes [18]. Hence, these compounds have been used as inductive agents for nerve cells to evaluate the neuroprotective ability of antioxidants. Although the pathways of action for neuroprotection by lignin have been reported, the structure-effect relationship between lignin and neuroprotection has not been investigated.

Grapes (*Vitis vinifera* L.) are one of the most widely cultivated fruits worldwide, and their cultivation area and yield have been ranked among the top for global fruit production for a long time. In 2018, the International Organization of the Vine and Wine pronounced that the international region for growing vines measures approximately 7 million hectares, which could produce ~78 million tons of grapes to produce wine [19]. Approximately 28% of the waste in industry is produced during wine production from grapes, and it contains 5% grape stalks and 23% grape seeds [20]. Lignin is rich in grape stalks and grape seeds, with concentrations of 32.9% [21] and 43% [20,22], respectively. Limited studies have investigated the biological activity of lignin obtained from grape seeds, particularly its neuroprotective effects [23]. Therefore, research conducted on protection against nerve cell damage by grape seed lignin should be further explored to enrich the biological value of lignin obtained from wine-making waste.

In this study, lignin samples in grape seeds with different substructures and functional groups were obtained by different technologies, which were designed to understand the effects of lignin fractions against BPAF neurotoxicity. Specifically, L-W was prepared from the autohydrolysate of grape seeds using resin purification. The lignins in the autohydrolyzed residue of grape seeds (L-R) and original grape seeds (L-O) were obtained using the classical milled wood lignin technique. The molecular weights, functional groups, and substructures of the prepared lignins were analyzed and characterized using gel permeation chromatography (GPC) and nuclear magnetic resonance (NMR). In addition, the antioxidant and neuroprotective properties of the prepared lignin were evaluated *in vitro* using murine neuroectodermal (NE-4C) stem cells induced using the BPAF. In addition, a preliminary study was conducted on grape seed lignin protection against BPAF-induced neurocyte injury, and this was evaluated with the apoptotic status and oxidation of NE-4C stem cells via the nuclear factor erythroid 2-related Factor 2 (Nrf2) pathway. Finally, the correlations between the physicochemical properties of grape seed lignins and their neural cell protective activities were evaluated using regression analysis. It is expected that this study will serve as a demonstration for obtaining active lignin from grape seed waste and thus improve grape seed waste utilization.

2 Experimental

2.1 Materials

Grape seeds were obtained from Urumqi Beiyuanchun Co., Ltd., Xinjiang, China. The grape seeds were milled to 80 mesh (average size < 0.18 mm) for further use. The grape seed samples were dewaxed with benzene/alcohol (2:1, v/v) mixtures for 10 h to remove lipids and then air-dried for 24 h before performing experiments.

NE-4C nerve cells were obtained from the mouse model and were provided by the School of Biomedical Engineering and Information, Nanjing Medical

University (Nanjing, China). BPAF (CAS 1478-61-1, purity 98%) was purchased from Shanghai Aladdin Biochemical Technology Co., Ltd. (Shanghai, China). A Cell Counting Kit-8 (CCK-8), Annexin V-FITC/PI Apoptosis detection kit, ROS assay kit, malondialdehyde (MDA) content assay kit, superoxide dismutase (SOD) activity assay kit, and mouse glutathione peroxidase (GSH-Px) ELISA kit were obtained from Nanjing YI FEI XUE Biotechnology Co., Ltd. (Nanjing, China). The reagents used in this study were of analytical grade.

2.2 Preparation of lignin from grape seeds

The protocol for obtaining lignin fractions from grape seeds is shown in the scheme in Fig. 1. Specifically, 5 g of ball-milled seed powder was dispersed in 50 mL of H_2O and then treated (autohydrolysis) at 170 °C for 60 min. The obtained slurry after autohydrolysis was centrifuged at 8000 r·min^{-1} for 5 min to obtain a suspension. The lignin in the autohydrolysate was adsorbed using polystyrene-divinylbenzene-glycidyl methacrylate (PS-DVB) resin (Amberlite® XAD 16N) to purify the lignin from the liquid supernatant by using the method of Huang et al. [24]. The purified lignin was termed L-W, and the residue was freeze-dried. The residues from autohydrolyzed and ball-milled grape seeds were extracted with dioxane and purified to obtain the L-R and L-O according to the classical method proposed by Björkman [25,26].

2.3 Analyses of the chemical compositions of grape seeds and lignin

The major components in raw grape seeds and lignin fractions were analyzed according to the standard National Renewable Energy Laboratory protocol [27]. Specifically, 0.3 g of powder (20–80 mesh) was initially immersed for 1 h in 72% (w/v) H_2SO_4 at room temperature before hydrolyzation with 4% (w/v) H_2SO_4 at 121 °C for 60 min. The released monosaccharides in the acid hydrolysate were analyzed using high-performance liquid chromatography (Agilent 1260 series, Agilent Technologies, USA) with an Aminex HPX-87H column and refractive index detector. A 5 mmol·L^{-1} H_2SO_4 solution was used as the eluent with a flow rate of 0.6 mL·min^{-1}.

2.4 Characterization of lignin

The molecular weight of lignin was determined by using GPC (Agilent 1100, Agilent Technologies, USA) and a PL-gel 10 mm mixed-B (inner diameter: 7.5 mm) column and UV detector. Subsequently, 0.004 g of lignin was added to tetrahydrofuran for analysis with elution conditions of 1.0 mL·min^{-1} and 25 °C.

Two-dimensional heteronuclear single quantum coherence (2D-HSQC) NMR spectra and quantitative ^{31}P NMR spectra of lignin were obtained with a Bruker 600 MHz NMR. Approximately 0.1 g of the lignin powder was dissolved in 0.5 mL of DMSO-d_6 for 2D-HSQC NMR. The ^{31}P NMR spectra were used to quantify the functional groups of lignin according to the study of Huang et al. [28]

2.5 Cell culture and biocompatibility evaluation *in vivo*

NE-4C cells were cultured in Dulbecco's modified Eagle's medium, which was supplemented with 100 units·mL^{-1}

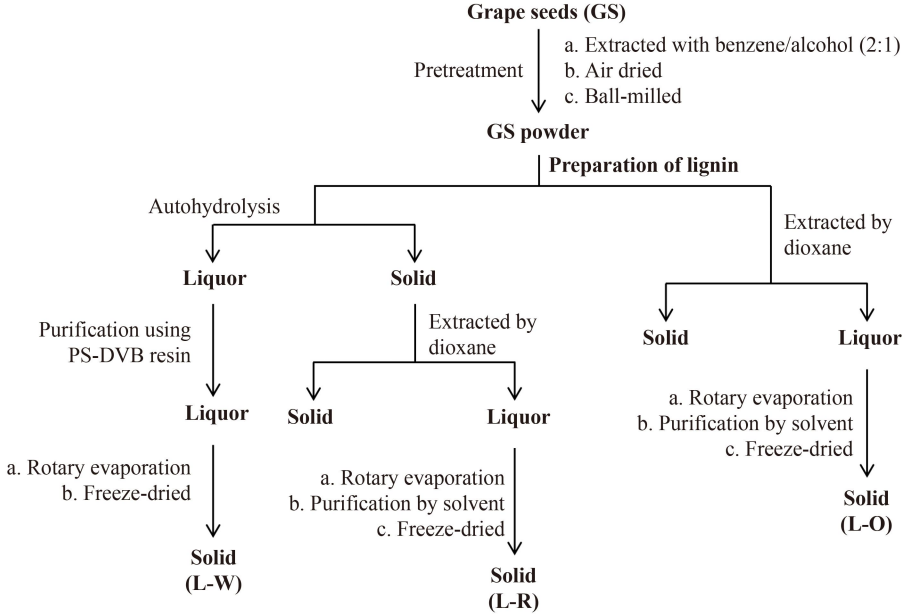

Fig. 1 Scheme for the isolation of lignin samples from grape seeds.

penicillin, 100 units·mL^{-1} streptomycin, and 10% (v/v) fetal bovine serum. The cells were kept at 37 °C in a humidified environment with 5% CO_2. Cell viability was determined with the CCK-8 assay. Specifically, NE-4C cells were cultured in 96-well plates (1×10^4 cells·well^{-1}) and exposed to various concentrations of BPAF (0.1, 0.5, 2, 10, 20, 40, and 60 μg·mL^{-1}) and lignin (25, 50, 100, 150, 200, and 400 μg·mL^{-1}, dimethyl sulfoxide solvent, and an equal dose of dimethyl sulfoxide was added to the control group) for 24 h. Subsequently, 10 μL of CCK-8 reagent was added to each well before incubation for 4 h at 37 °C, and the spectrophotometric absorbance at 450 nm was measured using a microplate reader. The results were expressed as the percentage of the control values compared with that of the control group.

2.6 Evaluation of the *in vitro* DPPH scavenging rate and antioxidant activities of lignin

To test the ability of lignin fractions to scavenge 2,2-diphenyl-1-picrylhydrazyl (DPPH), 2 mL of 0.2 mmol·L^{-1} DPPH solution (diluted in ethanol) was combined with lignin samples at different concentrations (50–500 μg·mL^{-1}) and left at 25 °C for 30 min in the dark. The control groups contained lignin devoid of DPPH, and the blank group was set up as the DPPH solution. After incubation, the solutions were transferred to 96-well plates. Then, a microplate reader was used to detect the spectrophotometric absorbance at 517 nm. The DPPH scavenging activity was calculated using Eq. (1):

$$\text{DPPH scavenging activity (\%)} = \left(1 - \frac{OD_{\text{test}} - OD_{\text{control}}}{OD_{\text{blank}}}\right) \times 100\%, \quad (1)$$

where OD_{test} is the OD value of the test groups which contained lignin and DPPH, OD_{control} is the OD value of the control groups which contained lignin devoid of DPPH, OD_{blank} is the OD value of the blank group which was set up as the DPPH solution.

A 6-well plate was filled with NE-4C cells (1×10^5 cells·mL^{-1}) and incubated for 24 h. The cells were then grown with BPAF or lignin fractions for 24 h. The obtained supernatants were collected after centrifugation of the medium. The production of reactive oxygen, MDA, SOD, and GSH-Px was measured using ELISA kits according to the protocols of the manufacturer. The experiments were performed thrice.

2.7 Neuroprotective properties of prepared lignin

NE-4C cells (1.5×10^5) were sown on confocal dishes and cultivated for 1 d before being incubated in fresh media. Subsequently, the NE-4C cells were treated with lignin fractions for 24 h according to the experimental procedure. The cells were fixed with 4% paraformaldehyde, incubated with 5% goat bovine serum to block nonspecific binding sites, and stained with Nrf2 mouse monoclonal antibody and Alexa Fluor 488-conjugated goat anti-mouse IgG to enable Nrf2 observation. Finally, the cells were stained with Hoechst 33342 dye before confocal laser scanning microscopy observation (LSM710, Zeiss Germany).

2.8 Statistical analyses

One-way analysis of variance was used to evaluate the data with SPSS software (Version 19.0 for Windows, SPSS Inc., Chicago, IL, USA). Tukey's multiple range tests were used to distinguish the means of the treatment groups. When $P < 0.05$, the data were assumed to be statistically significant.

3 Results and discussion

3.1 Composition analysis of prepared lignin fractions

In this study, grape seeds were used to prepare different lignin fractions and evaluate their biological activities. Table 1 shows that grape seed contains a significant proportion of lignin (58.16%) and a small amount of carbohydrate (6.34%). The higher proportion of lignin in grape seeds compared with hardwood (18%–25%), softwood (25%–35%), and grassy biomass (10%–30%) [29] indicated that grape seeds can be used as a lignin-rich substrate from which to obtain lignin fractions with various structures. The L-W in the autohydrolysate from grape seeds, L-R in autohydrolyzed grape seeds, and L-O in grape seeds were obtained and purified into lignin fractions with different structural properties. The compositions of these lignin fractions are shown in Table 1. It was demonstrated that both lignin fractions contained high proportions of lignin (> 75%), which indicated that there were sufficient samples to further analyze the structural properties and biological activities.

Table 1 Composition of grape seed and lignin fractions from grape seeds

Item	Sugar content/%					Acid insoluble lignin content/%	Acid soluble lignin content/%
	Araban	Galactan	Glucan	Xylan	Mannan		
Seeds	0.40	0.43	1.72	2.96	0.83	53.00	5.16
L-W	4.85	0.04	0.20	7.66	0.10	60.00	16.14
L-R	0.02	0.01	2.46	0.04	0.06	74.00	3.84
L-O	0.16	0.14	1.51	0.14	0.57	70.33	15.25

Although purification techniques were used in this study to obtain different lignin fractions, some carbohydrates was present in the purified lignin fractions. The carbohydrates observed in the lignin fractions were in lignin-carbohydrate complexes (LCCs) formed by covalent bonds, which were not degraded by organic solvents during the purification process. Additionally, it was observed that abundant LCC fractions were present in the purified L-W obtained from hardwood prehydrolysate [30] and original lignin from mill-wood lignin in bamboo [31]. Xylan was the predominant carbohydrate present in the lignin fractions from the L-W treatment (59.61%), whereas glucan was the predominant sugar component in the L-R and L-O treatments, with proportions of 94.98% and 58.30%, respectively. The difference in sugar components observed in these fractions can be explained by the fact that xylan is the major carbohydrate in grape seeds, and it is more easily degraded to form LCCs than glucan during autohydrolysis [32]. The major component in the cell walls of autohydrolyzed and L-O was glucan, which was covalently linked with lignin and could not be completely eliminated during purification with an organic solvent. NMR studies were performed to reveal the features of LCCs in the L-W, L-R, and L-O fractions and confirm this speculation.

3.2 Analyses of the molecular weights of the prepared lignin fractions

To ascertain the molecular weights of the lignin fractions prepared from grape seeds, GPC curves were used to derive the weight-average molecular weights (M_w) and number-average molecular weights (M_n). Table 2 shows that the L-O in grape seeds had M_w and M_n values of 4750 and 2390 g·mol^{-1}, respectively, which were slightly higher than the molecular weights of the original lignin obtained from grape stalks (~2600 g·mol^{-1}) in the study conducted by Prozil et al. [21]. In the case of the L-W and L-R lignin fractions, the molecular weights, with M_w values of 3830 and 900 g·mol^{-1}, respectively, were lower than that of L-O. This may be due to degradation of the substructures in lignins during the autohydrolysis process, which might have resulted from degradation of β-O-4 ethers by hydrogen ions [33]. In addition, both prepared lignin fractions had narrow molecular weight distributions with polydispersity index values (M_w/M_n) lower than 2. The results in Table 2 indicate that the prepared lignin fractions L-W, L-R, and L-O possessed different molecular weights, which can be used to prepare lignin fractions with various properties when evaluating their biological activities.

Table 2 M_w, M_n, and polydispersity indexes (*PDI*) of L-W, L-R, and L-O

Item	M_w/(g·mol^{-1})	M_n/(g·mol^{-1})	*PDI* [a]
L-W	900	670	1.34
L-R	3830	2350	1.63
L-O	4750	2390	1.99

a) *PDI*: polydispersity index (M_w/M_n).

3.3 Structural characterization of prepared lignin fractions with NMR

The biological ability of lignin is related to its structural properties, such as the number of linkages in the subunits and the content of functional groups [34]. The structural features of the lignin fractions L-W, L-R and L-O were revealed by using the 2D-HSQC NMR technique to identify the existing linkages and lignin units. The 2D-HSQC spectra and the main substructures are shown in Fig. 2.

The primary substructures β-O-4 (A) and β-β (B) in the lignin fractions were observed in regions δ_C/δ_H 90–50/6.0–2.5 in the HSQC spectra. The C_a-H_a and C_β-H_β correlations for β-O-4 were specifically found at δ_C/δ_H 72.4/4.62 and 83.2/3.82, respectively. For β-β, the C_a-H_a and C_β-H_β correlations were found at δ_C/δ_H 83.9/4.49 and 53.5/3.11, respectively. Generally, two types of β-O-4 substructures were observed in the 2D-HSQC spectra of lignin obtained from grassy biomass, which were linked to guaiacyl (A_β (*G*)) and syringyl units (A_β (*S*)) [14]. However, only the signals for A_β (*G*) were present in the spectra of L-W, L-R, and L-O, which indicated that *S* units were absent from the lignin of grape seeds. This speculation was proven by the signals in the regions δ_C/δ_H 150–90/9.0–4.5 in the HSQC spectra, in which only syringyl (*S*) units and *p*-hydroxyphenyl (*H*) units were detected. Specifically, the C–H correlations of C_2–H_2, C_5–H_5, and C_6–H_6 in syringyl (*S*) units were observed at δ_C/δ_H 109.5/6.91, δ_C/δ_H 115.1/6.70, and δ_C/δ_H 119.0/6.69, respectively. The signals at δ_C/δ_H 128.9/7.21 were attributed to $C_{2,6}$–$H_{2,6}$ in the *p*-hydroxyphenyl (*H*) units.

2D-HSQC signals for the carbohydrates β-(1→4)-D-xylopyranoside (X) and β-(1→4)-D-xylopyranoside with a non-reducing end (X_{NR}) were identified with the corresponding C–H correlations. The presence of these carbohydrates was due to the presence of LCCs in the lignin fractions. The benzyl ether (BE) and phenyl glycoside (PhGlc) LCC linkages were identified from the 2D-HSQC spectra with δ_C/δ_H 85–75/5.3–4.3 and δ_C/δ_H 105–90/5.3–4.0, respectively. Three types of PhGlc were identified in the L-W spectra from their signal intensities. In contrast, these signals were weak in the spectra of L-O and absent from the spectra of L-R. This resulted because the linkages in PhGlc were susceptible to degradation during the autohydrolysis process, which resulted in a lower proportion of PhGlc in the residual lignin in grape seeds.

L-W, L-R and L-O had similar substructures and lignin units, whereas the types of LCCs in these lignin fractions were different. The contents of lignin substructures and

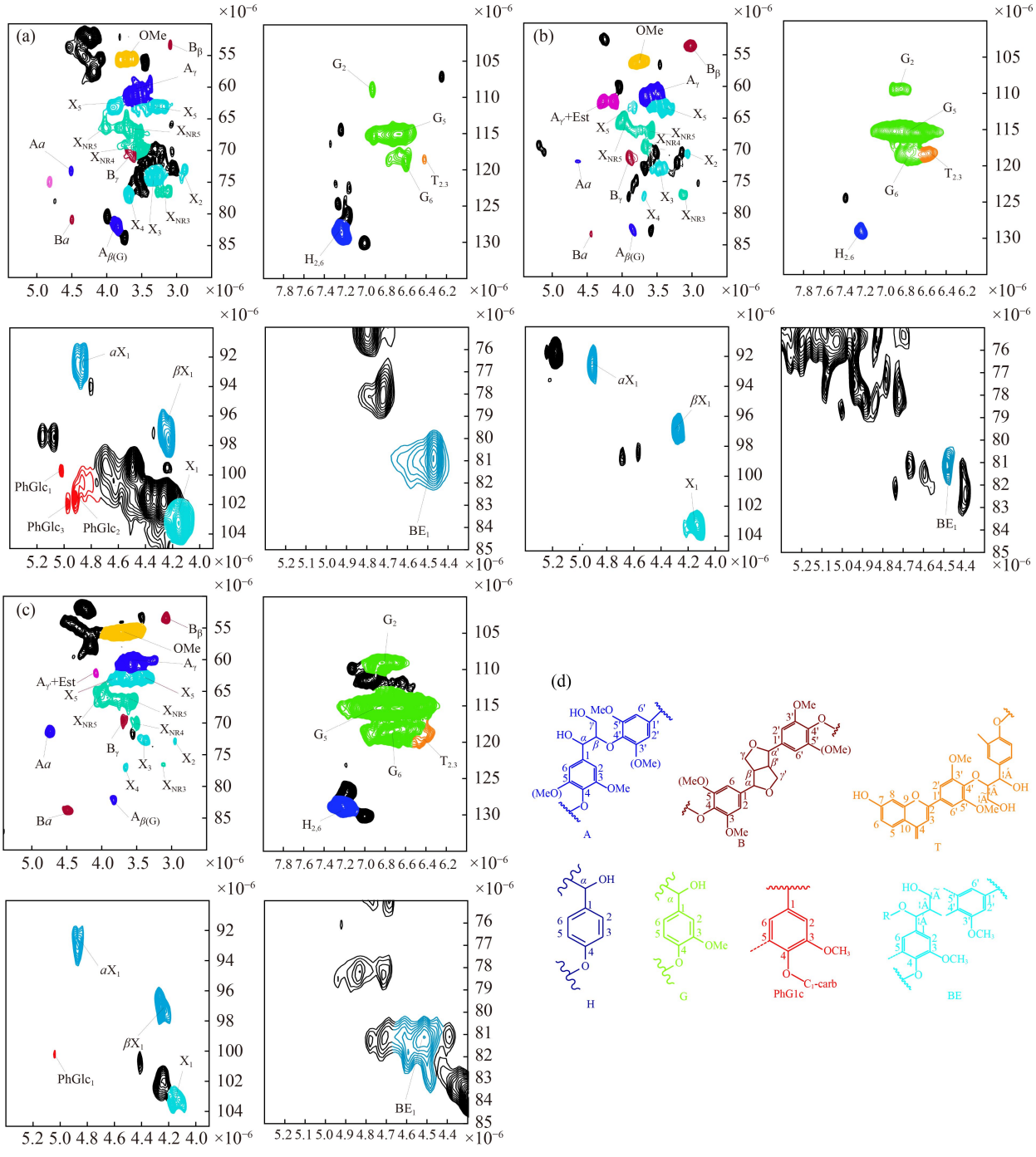

Fig. 2 HSQC spectra of (a) L-W, (b) L-R, (c) L-O and (d) the main structures contained in the lignin preparations.

LCCs in L-W, L-R and L-O were calculated based on their signal intensities in 2D-HSQC spectra. The quantitative results based on 100 Ar (C900) are listed in Table 3. L-O contained higher *β*-O-4 and *β*-*β* contents than L-W and L-R, with 30.1/100 Ar and 21.9/100 Ar, respectively. In the case of LCC linkages, L-O had a higher BE (24.9/100 Ar) content than L-W (18.4/100 Ar) and L-R (8.1/100 Ar). The decreased proportions of lignin interunit linkages and LCC linkages in L-W and L-R indicated that these linkages were degraded during the autohydrolysis process. A study conducted by Gu et al. [35] demonstrated that autohydrolysis degraded the linkages in lignin structures and LCCs, which was used to prepare lignin fractions with different structural features and analyze their biological activities.

The antioxidative properties of lignin enable biological activities such as scavenging ROS and antibacterial and antiviral properties. Generally, the functional groups determine the antioxidative ability of lignin [10–12]. Hence, the number of functional groups in L-W, L-R, and

L-O were quantitatively analyzed using the ^{31}P NMR technique, and the results are shown in Table 3.

The phenolic hydroxyl content of the L-O in grape seeds was 2.8 mmol·g^{-1}, which was slightly lower than those of L-W (3.0 mmol·g^{-1}) and L-R (3.1 mmol·g^{-1}), as shown in Table 3. This was due to degradation of β-O-4 linkages in the L-O from grape seeds during the autohydrolysis process, which increased the content of phenolic hydroxyl groups in fractionated lignin in the autohydrolysate (L-W) and pretreated substrate (L-R). Generally, the number of aliphatic hydroxyl groups in lignin was negatively correlated with its molecular weight [36]. Table 3 shows that L-W, with the lowest M_w, had the highest content of aliphatic hydroxyl groups. This was explained by the fact that L-W contained a significant proportion of carbohydrates in its inherent structure, which was determined by ^{31}P NMR spectral data for the aliphatic hydroxyl region. The overlap of signals for the hydroxyl groups in carbohydrates with the aliphatic hydroxyl signals from lignin in L-W resulted in determination of a deceptive content of aliphatic hydroxyl groups of L-W. It was reported that a higher content of phenolic hydroxyl groups and a certain proportion of accompanying carbohydrates in the lignin structure endow lignin with a higher antioxidant capacity to eliminate free radicals and ROS [34,37]. Hence, it was speculated that L-W possessed a higher antioxidant ability and biological activity than L-R and L-O.

Table 3 Proportions of lignin substructures, LCC linkages, and functional groups in lignin fractions obtained from grape seeds

Characteristics	L-W	L-R	L-O
Lignin substructures (100 Ar)			
β-O-4 (A)	12.8	14.2	30.1
β-β (B)	10.2	9.8	21.9
LCC linkages (100 Ar)			
Benzyl ether (BE)	18.4	8.1	24.9
Phenyl glycoside (PhGlc)	6.2	0	2.1
Total	24.6	8.1	27.0
Functional groups (mmol·g^{-1})			
Aliphatic hydroxyl	7.7	1.9	3.8
Noncondensed phenolic hydroxyl	3.0	3.1	2.8
COOH	0.9	0.7	1.2

3.4 Biocompatibility of lignin and BPAF in NE-4C cells and their effects on apoptosis

Biocompatibility is a crucial indicator that should be considered for bioactive agents because it might affect their interactions with cells and organisms. Hence, the biocompatibilities of lignin fractions obtained from grape seeds were evaluated for NE-4C neuronal cells with the CCK-8 experiment. In addition, cells were stimulated with different concentrations of BPAF to determine the damaging effects of BPAF on the viability of NE-4C cells with a CCK-8 assay. The viability of NE-4C cells after treatment with BPAF and lignin is shown in Fig. 3. Figure 3(a) shows that the half maximal inhibitory concentration (IC50) for cells was obtained when the BPAF concentration was 16 μg·mL^{-1}. Hence, 15 μg·mL^{-1} BPAF was selected for further assays used to investigate the recovery capability of different lignin fractions with BPAF-treated NE-4C neuronal cells. Evaluations of cytotoxicity of the three lignin fractions for NE-4C cells (Fig. 3(b)) showed that the cellular viability initially increased upon increasing the L-W concentration from 25 to 50 μg·mL^{-1} and subsequently decreased with further increases in the L-W concentration from 50 to 400 μg·mL^{-1}. Increases in the concentrations of L-R and L-O from 25 to 400 μg·mL^{-1} gradually decreased cellular viabilities, which were lower than that seen with L-W. This indicated that the cytotoxicities of L-R and L-O were higher than that of L-W. Figure 3(b) shows that the cell activity was approximately 110% when the concentrations of L-W, L-R, and L-O were 25 μg·mL^{-1}. This concentration was nontoxic and promoted proliferation. Therefore, 25 μg·mL^{-1} was selected as the processing concentration of different lignin fractions for further assays.

The biological effects of different lignin fractions and recovery capacity for BPAF-induced neuronal cells of

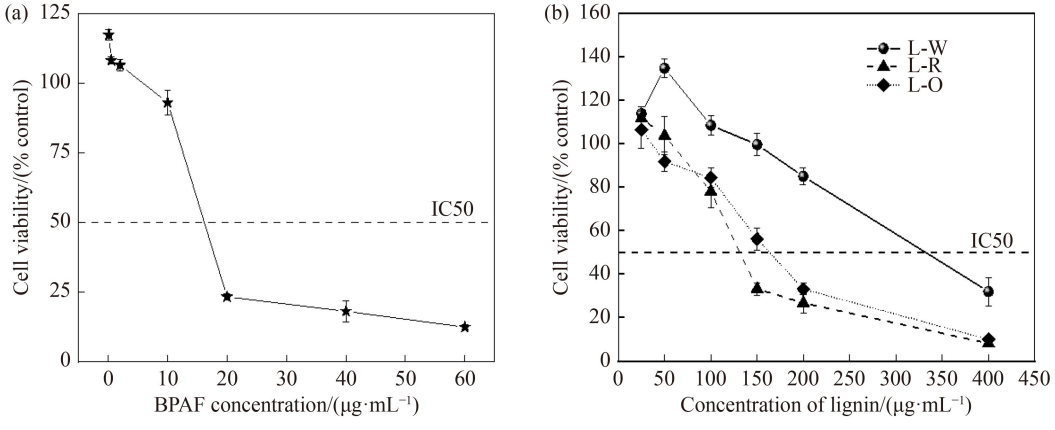

Fig. 3 Cell viabilities of NE-4C cells after treatment with (a) BPAF and (b) lignin.

NE-4C were evaluated with the apoptosis model. The cells were initially treated with 15 μg·mL^{-1} BPAF and subsequently treated with 25 μg·mL^{-1} L-W, L-R, and L-O for 24 h. Microphotographs, flow cytometry results of cell apoptosis and the relative apoptosis rates of NE-4C cells after incubation with BPAF and different lignins are shown in Fig. 4. Images indicating cell status and apoptosis rate are shown in Figs. 4(a) and 4(b), respectively. Figure 4(a) shows that the NE-4C cells exhibited the morphology of extended cytoplasm and filopodia in the control group and the groups with L-W, L-R, and L-O fractions. This indicated that the cells actively attached to the surfaces of the culture dishes, particularly in the L-W, L-R, and L-O groups. Moreover, the number of NE-4C cells was significantly increased, which indicated the proliferation-promoting ability of lignin in neuronal cells. In the case of the BPAF-induced group, it was observed that a few of the cells had oval shapes without filopodia and were suspended in the medium, which represented a floating state of death. This revealed that treatment with the bisphenol compounds BPA and BPAF resulted in toxicity for neuronal cells, which was in accordance with the study conducted by Huang et al. [38]. Although a few dead cells were present, L-W, L-R, and L-O exhibited different protective capabilities allowing damaged cells to return to the normal state after the lignin fractions were added to the BPAF-treated cells. Figures 4(b) and 4(c) show that the apoptosis rate of NE-4C cells treated with 15 μg·mL^{-1} BPAF was 182.11%, while treatments with lignin fractions at 25 μg·mL^{-1} significantly reduced the apoptosis rates of BPAF-treated cells from 182.11% to 128.90% (L-W), 121.10% (L-R), and 147.71% (L-O); this showed that L-R outperformed L-W and L-O. A study conducted by Gu et al. [39] demonstrated that LCCs from different biomasses improved the antioxidant activity of BPA-induced nerve damage in zebrafish, which demonstrated that lignin-derived polymers have neuroprotective properties. The protective effects of lignin fractions with different structures toward BPAF-induced neurotoxicity of NE-4C cells have not been demonstrated. Therefore, the following section assesses the connections between structural characteristics of lignin fractions and their neuroprotective qualities.

3.5 Lignin scavenging effect on BPAF-induced ROS production in NE-4C cells

The scavenging ability of BPAF-induced NE-4C cells was evaluated *in vitro* at a biosafety concentration to further understand the effect of lignin fractions on the recovery capability of NE-4C cells. The scavenging activity of L-W for DPPH was greater than those of L-R and L-O, as shown in Fig. 5(a). The IC50-DPPH value (the concentration of lignin required to scavenge 50% of the DPPH *in vitro*) of L-W (58.19 μg·mL^{-1}) was lower than those of L-R (84.27 μg·mL^{-1}) and L-O (99.44 μg·mL^{-1}). In addition, the IC50-DPPH of L-O had the highest scavenging activity compared with that of DPPH of L-O. These results demonstrated that L-W from the autohydrolysate had a lower IC50-DPPH than the original lignin in the cell walls of biomass. Studies by Wang et al. [14] and Yun et al. [40] demonstrated that the L-W from bamboo had a higher antioxidant ability than the bamboo kraft lignin prepared by organosolv fractionation. Table 4 compares the DPPH scavenging capacities (based on IC50 values) reported earlier for lignins from different plants [14,40–42]. It was found that L-W, L-R, and L-O exhibited good antioxidant capacities at lower dosages, indicating that the lignin fractions from grape seeds may show good biological activity when intervening in a disease regulated by free radicals and ROS.

Generally, stimulation of neurotoxic chemicals, such as di-2-ethylhexyl phthalate, BPA, and its derivatives (BPA, BPAF, BPF, and BPS), could result in a stressed state of the cell and activate the cellular antioxidant system [39,43]. The levels of representative antioxidant chemicals are decreased during external stimulation, and the cellular antioxidant system is broken [44]. It was observed in the abovementioned studies that L-W, L-R, and L-O possessed antioxidative properties.

The major antioxidant indices ROS, MDA, SOD, GSH-Px, and Nrf2 in BPAF-treated NE-4C cells were measured after treatment with different lignin fractions to understand their neuroprotective properties via the antioxidant pathway, and the results are shown in Fig. 5. Figure 5(b) shows that treatment with BPAF significantly enhanced the ROS levels and MDA content and reduced the SOD and GSH-Px activities of normal NE-4C cells. L-W, L-R, and L-O showed strong capacities for reducing ROS levels, which indicated their ability to scavenge ROS. These results were consistent with the results shown in Fig. 5(a). L-W more effectively suppressed ROS production compared with L-R and L-O when these lignins were coincubated with BPAF-treated NE-4C cells (Fig. 5(b)). Generally, the MDA content is an indication of the degree of peroxidation of the cell membrane [45]. A high MDA content indicates a high degree of peroxidation and severe damage to the cell membrane. Membrane peroxidation generally occurs under adverse conditions such as high temperature, salinity, or toxicity [46]. The MDA content results in Fig. 5(c) demonstrated that the 25 μg·mL^{-1} lignin fractions did not damage cell membranes. Moreover, the lignin fractions protected the cells from BPAF-induced damage by reducing the MDA content. In addition, the induction of BPAF significantly reduced the SOD and GSH-Px activities of NE-4C cells (Fig. 5(d)). Figure 5(d) shows that the three lignin fractions improved the SOD activity in NE-4C cells, which reestablished the SOD activity of NE-4C cells inhibited by BPAF. Figure 5(e) shows that treatment of

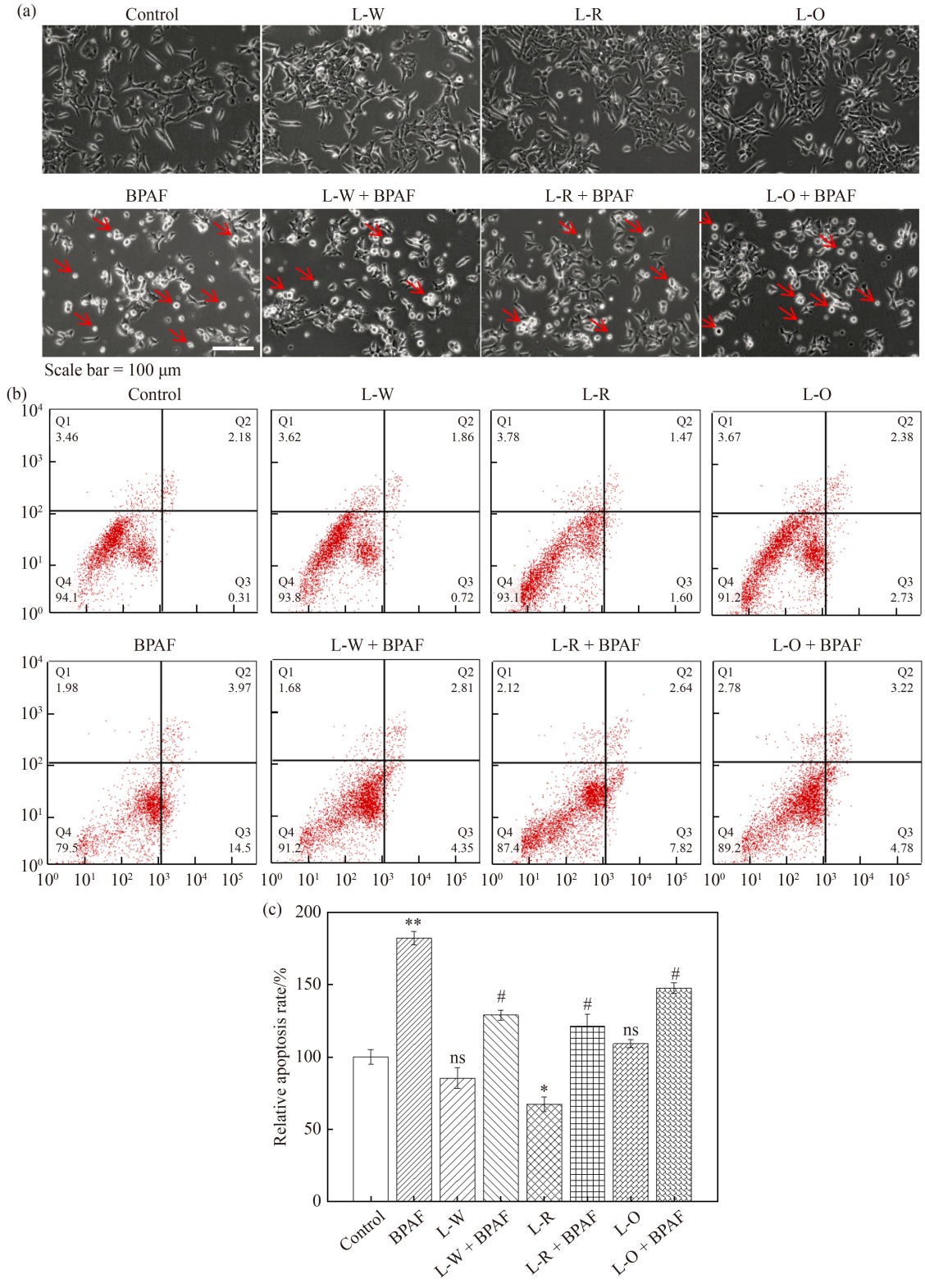

Fig. 4 (a) Microphotographs, (b) flow cytometry results of cell apoptosis and (c) relative apoptosis rates for NE-4C cells after incubation with BPAF and different lignins. * $0.01 < p < 0.05$, ** $p < 0.01$, compared with the control group. # $0.01 < p < 0.05$, compared with BPAF treatment alone.

NE-4C cells with individual lignins did not significantly increase cellular GSH activity, whereas L-W, L-R, and L-O significantly increased the GSH-Px activity of BPAF-induced NE-4C cells. These results were supported by the research conducted by Zheng et al. [34], which demonstrated that three fractions with different molecular

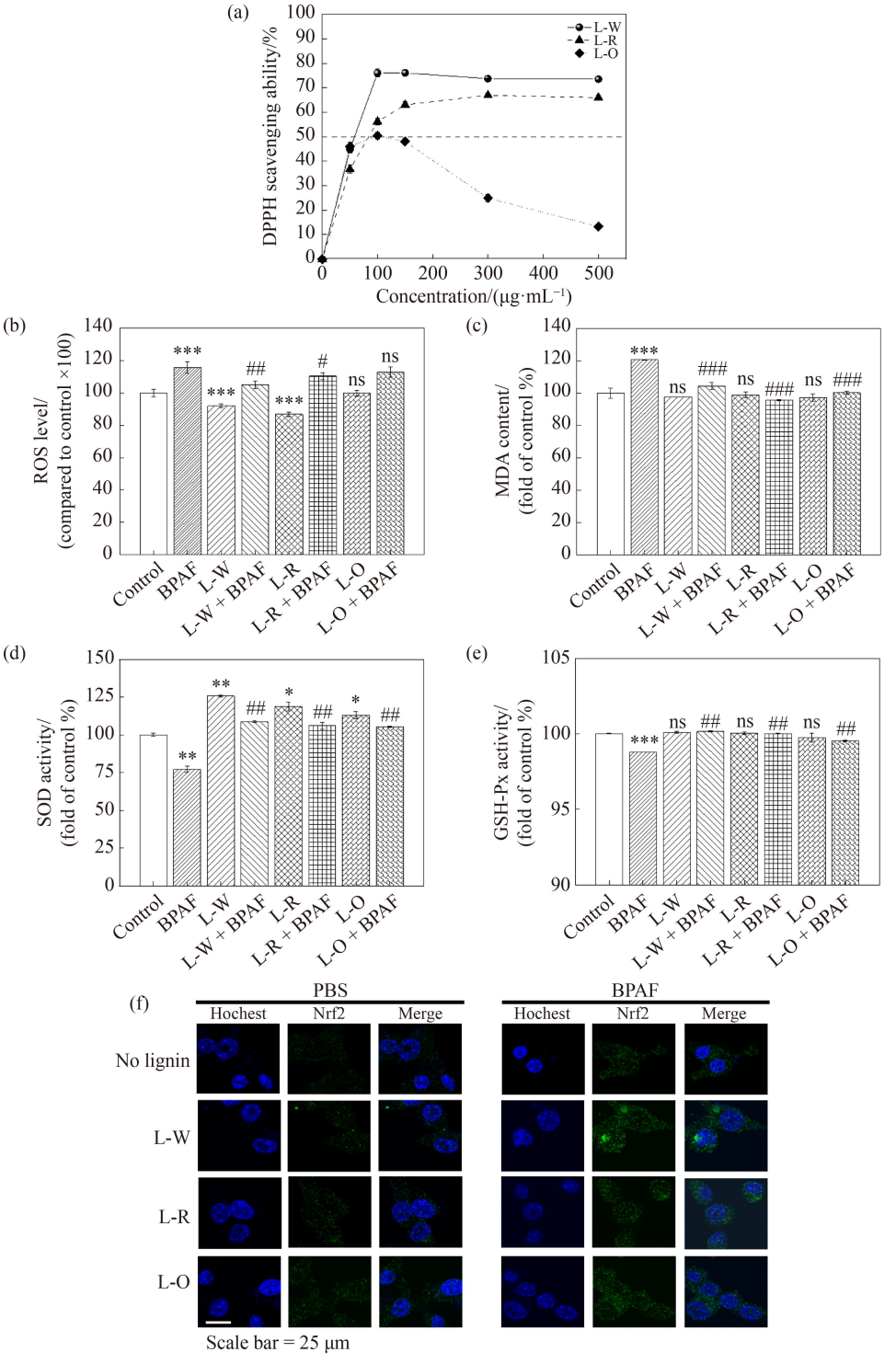

Fig. 5 Effects of L-W, L-R and L-O on BPAF-induced oxidative stress in NE-4C cells. (a) DPPH scavenging ability; (b) flow cytometry results for generated ROS; (c) MDA content; (d) SOD activity; (e) GSH-Px activity; (f) Nrf2 level. * $0.01 < p < 0.05$, ** $p < 0.01$, *** $p < 0.001$, compared with the control group. # $0.01 < p < 0.05$, compared with BPAF treatment alone. ## $p < 0.01$, compared with BPAF treatment alone. ### $p < 0.001$, compared with BPA treatment alone.

weights exhibited different substructures and antioxidant abilities. The aforementioned results show that the cellular antioxidant ability of lignin fractions with BPAF-treated NE-4C cells might be attributable to their neuroprotective properties.

Nrf2 is a nuclear transcription factor associated with oxidative stress, and it has been observed that several natural products with antioxidant activity are cytoprotective by activating Nrf2 [47]. Hence, the levels of Nrf2 in the BPAF-induced NE-4C cells treated with different

lignin fractions were analyzed further. The green fluorescence (representing Nrf2) in Fig. 5(f) demonstrates that the three lignin fractions increased the fluorescence intensity of Nrf2 in PBS-treated NE-4C cells and BPAF-treated NE-4C cells, particularly in the groups of NE-4C cells treated with BPAF. These results suggested that L-W, L-R, and L-O increased the level of Nrf2, which indicated that activation of the Nrf2 pathway was involved in the neuroprotective functions of the lignin fractions.

3.6 Regression analysis of the connections between the biological properties of lignin fractions and the substructures

Generally, the biological activity of lignin is closely related to its molecular weight, the numbers of hydroxyl and carboxyl groups, and other structural properties. To further comprehend the connection between the physicochemical properties of the three lignin fractions (L-W, L-R, and L-O) and their various neuroprotective capabilities, Pearson's test was used to calculate the reliability coefficients for the structure-activity relationships of lignin. A heatmap of the lignin structure and the antioxidant index are depicted in Fig. 6. This showed that M_w, M_n, and PDI exhibited positive correlations with the scavenging rates for DPPH (p values of 0.99, 0.94, and 0.97, respectively) and ROS (p values of 0.34, 0.13, and 0.65, respectively), which showed negative correlations with IC50 of the lignin (p values of –0.93, –0.99, and –0.73, respectively), SOD activities (p values of –0.97, –0.90, and –0.99, respectively) and GSH-Px activities (p values of –0.81, –0.66, and –0.96, respectively). Specifically, lignins with lower molecular weights exhibited greater capacities to scavenge ROS and encouraged synthesis of antioxidant enzymes in NE-4C cells. However, they exhibited greater toxicity toward cells. Zheng et al. [34], Yang et al. [48], and Liu et al. [4] evaluated the DPPH scavenging ability of lignins extracted from different biomasses and observed that the DPPH scavenging ability showed a negative correlation with M_w. A linear relationship existed between M_w and the DPPH scavenging rate, which indicated that the M_w of the lignin had a strong negative correlation with its ability to scavenge ROS. Additionally, the combined β-O-4 and β-β content had positive correlations with the DPPH scavenging rate and ROS and negative correlations with the IC50 of lignin, MDA content, and SOD and GSH-Px activities. These results were supported by the study conducted by Zheng et al. [34].

Figure 6 also shows that the content of noncondensed phenolic hydroxyl groups exhibited a significant negative correlation with ROS scavenging ability ($r = -1$) and a significant positive correlation with the ability of lignin to regulate MDA ($r = 0.91$) and GSH-Px activity ($r = 0.87$). Additionally, the studies conducted by Yao et al. [10] and Zhang et al. [49] showed that the phenolic hydroxyl group content of the lignin plays a crucial role in

Table 4 IC50 values for different lignins in previously reported work compared to the lignin fractions from grape seeds

Lignins	IC50-DPPH/(μg·mL^{-1})	Reference
Grape seeds (L-W)	58.19	This work
Grape seeds (L-R)	84.27	This work
Grape seeds (L-O)	99.44	This work
Moso bamboo	314	[13]
Wheat stalk	402	[13]
Moso bamboo	290	[38]
Conocarpus erectus leaves	231.16	[39]
Cornstalk	88.20	[40]

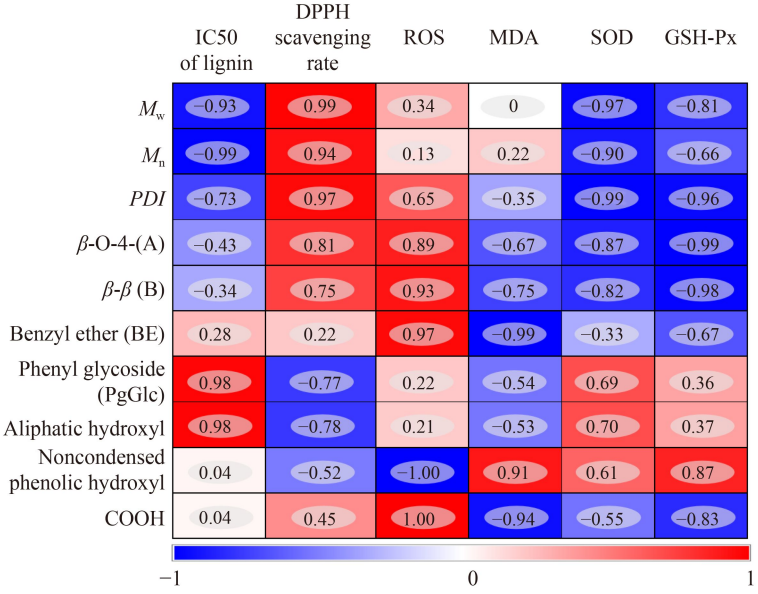

Fig. 6 Connections between the biological properties of lignin fractions and the substructures. Red represents a positive relationship, and blue represents a negative relationship.

scavenging ROS *in vivo* or *in vitro*. The COOH content and the noncondensed phenolic hydroxyl groups demonstrated contrasting phenomena. Specifically, the COOH content had a significant positive correlation with ROS scavenging ability (r = 1) and a significant negative correlation with MDA (r = −0.94) and GSH-Px activity (r = −0.83). This result was validated by the study of Na et al. [50], who reported that the hydrophilic COOH groups of lignin generate its ability to scavenge ROS. The proportions of noncondensed phenolic hydroxyls and COOH groups did not exhibit a correlation with the IC50 of lignin (r = 0.04). It was demonstrated that the lignin fraction properties M_w, M_n, PDI, β-O-4, β-β, noncondensed phenolic hydroxyl, and COOH regulated the neuroprotective activities of lignin fractions for BPAF-induced neuronal cells. Free radicals are generated by cells during metabolic processes and are involved in signal transduction, gene expression, and activation of various receptors [51]. Stimulation from BPAF can induce an increase in free radicals in NE-4C cells and generate oxidative stress. It has been reported that lignin preparations with high β-O-4 bond, β-β bond, BE, and –COOH contents can effectively stimulate the oxidative stress responses of neuronal cells. In particular, the carboxyl content in the lignin structure plays a significant and positive role in scavenging ROS, which can protect against BPAF-induced neuronal cell injury [34,35].

4 Conclusions

The three lignin fractions L-W, L-R, and L-O with different physical and chemical properties were prepared from grape seeds by using different techniques. NMR characterizations demonstrated that the grape seed lignin possessed *S* and *H* subunits and β-O-4 and β-β substructures. A strong relationship was observed between the physicochemical properties of L-W, L-R, and L-O and their different neuroprotective abilities due to their ability to activate the Nrf2 pathway. Specifically, in the case of L-W with lower molecular weights, a lower content of noncondensed phenolic hydroxyl groups and a higher content of COOH groups ensured effective cell apoptosis inhibition, ROS scavenging, and nerve injury protection of BPAF-treated neuronal cells. This demonstrated its potential as an efficient neuroprotective agent.

Acknowledgments This work was sponsored by the National Natural Science Foundation of China for Youth (Grant No. 81901873), the Jiangsu Qing Lan Project (for Dr. Caoxing Huang) and the Young Elite Scientists Sponsorship Program by CAST (for Dr. Caoxing Huang).

References

1. Hu T Q. Chemical Modification, Properties, and Usage of Lignin. New York: Kluwer academic/Plenum publishers, 2002: 81–82
2. Liu H Y, Xu T, Liu K, Zhang M, Liu W, Hao L, Du H S, Si C L. Lignin-based electrodes for energy storage application. Industrial Crops and Products, 2021, 165: 113425
3. Chen Z S, Yan M, Pei W, Yan B, Huang C, Chan H Y E. Lignin-carbohydrate complexes suppress SCA3 neurodegeneration via upregulating proteasomal activities. International Journal of Biological Macromolecules, 2022, 218: 690–705
4. Liu K, Du H S, Zheng T, Liu W, Zhang M, Liu H Y, Zhang X Y, Si C L. Lignin-containing cellulose nanomaterials: preparation and applications. Green Chemistry, 2021, 23: 9723–9746
5. Pei W, Deng J, Wang P, Wang X, Zheng L, Zhang Y, Huang C. Sustainable lignin and lignin-derived compounds as potential therapeutic agents for degenerative orthopaedic diseases: a systemic review. International Journal of Biological Macromolecules, 2022, 212: 574–560
6. Shao Z, Fu Y, Wang P, Zhang Y, Qin M, Li X, Zhang F. Modification of the aspen lignin structure during integrated fractionation process of autohydrolysis and formic acid delignification. International Journal of Biological Macromolecules, 2020, 165: 1727–1737
7. Pu Y, Hu F, Huang F, Ragauskas A J. Lignin structural alterations in thermochemical pretreatments with limited delignification. BioEnergy Research, 2015, 8: 992–1003
8. Lagerquist L, Pranovich A, Sumerskii I, Schoultz S V, Vähäsalo L, Willför S, Eklund P. Structural and thermal analysis of softwood lignins from a pressurized hot water extraction biorefinery process and modified derivatives. Molecules, 2019, 24: 335
9. Lagerquist L, Pranovich A, Smeds A, Schoultz S, Vähäsalo L, Rahkila J, Kilpeläinen I, Tamminen T, Willför S, Eklund P. Structural characterization of birch lignin isolated from a pressurized hot water extraction and mild alkali pulped biorefinery process. Industrial Crops and Products, 2018, 111: 306–316
10. Yao L, Xiong L, Yoo C G, Dong C, Meng X, Dai J, Ragauskas A J, Yang C, Yu J, Yang H, Xiong C. Correlations of the physicochemical properties of organosolv lignins from Broussonetia papyrifera with their antioxidant activities. Sustainable Energy & Fuels, 2020, 4: 5114–5119
11. Dizhbite T, Telysheva G, Jurkjane V, Viesturs U. Characterization of the radical scavenging activity of lignins-natural antioxidants. Bioresource Technology, 2004, 95: 309–317
12. Liu H Y, Xu T, Cai C Y, Liu K, Liu W, Zhang M, Du H S, Si C L, Zhang K. Multifunctional superelastic, superhydrophilic, and ultralight nanocellulose-based composite carbon aerogels for compressive supercapacitor and strain sensor. Advanced Functional Materials, 2022, 32: 2113082
13. Liu W, Liu K, Du H S. Zheng, Zhang N, Xu T, Pang B, Zhang X Y, Si C L, Zhang K. Cellulose nanopaper: fabrication, functionalization, and applications. Nano-Micro Letters, 2022, 14: 104
14. Wang R, Zheng L, Xu Q, Xu L, Wang D, Li J, Lu G, Huang C, Wang Y. Unveiling the structural properties of water-soluble lignin from gramineous biomass by autohydrolysis and its functionality as a bioactivator (anti-inflammatory and

antioxidative). International Journal of Biological Macromolecules, 2021, 191: 1087–1095
15. Park S Y, Park S J, Park N J, Joo W H, Lee S J, Choi Y W. α-Iso-cubebene exerts neuroprotective effects in amyloid beta stimulated microglia activation. Neuroscience Letters, 2013, 555: 143–148
16. Song F, Zeng K, Liao L, Yu Q, Tu P, Wang X. Schizandrin a inhibits microglia-mediated neuroninflammation through inhibiting TRAF6-NF-κB and Jak2-Stat3 signaling pathways. PLoS One, 2016, 11: e0149991
17. Zhou F, Wang M, Ju J, Wang Y, Liu Z, Zhao X, Yan Y, Yan S, Luo X, Fang Y. Schizandrin A protects against cerebral ischemia-reperfusion injury by suppressing inflammation and oxidative stress and regulating the AMPK/Nrf2 pathway regulation. American Journal of Translational Research, 2019, 11: 199–209
18. Gu J, Zhang J, Chen Y, Wang H, Guo M, Wang L, Wang Z, Wu S, Shi L, Gu A, et al. Neurobehavioral effects of bisphenol S exposure in early life stages of zebrafish larvae (Danio rerio). Chemosphere, 2019, 217: 629–635
19. OIV. 2019 Statistical Report on World Vitiviniculture. International Organisation of Vine and Wine. Available online: 2019
20. Yedro F M, Serna J G, Cantero D A, Sobrón F, Cocero M J. Hydrothermal fractionation of grape seeds in subcritical water to produce oil extract, sugars and lignin. Catalysis Today, 2015, 257: 160–168
21. Prozil S O, Evtuguin D V, Silva A M S, Lopes L P C. Structural characterization of lignin from grape stalks (*Vitis vinifera* L.). Journal of Agricultural and Food Chemistry, 2014, 62: 5420–5428
22. Spanghero M, Salem A Z M, Robinson P H. Chemical composition, including secondary metabolites, and rumen fermentability of seeds and pulp of Californian (USA) and Italian grape pomaces. Animal Feed Science and Technology, 2009, 152: 243–255
23. Vostrejs P, Adamcová D, Vaverková M D, Enev V, Kalina M, Machovsky M, Šourková M, Marova I, Kovalcik A. Active biodegradable packaging films modified with grape seeds lignin. RSC Advances, 2020, 10: 29202–29213
24. Huang C, Wang X, Liang C, Jiang X, Yang G, Xu J, Yong Q. A sustainable process for procuring biologically active fractions of high-purity xylooligosaccharides and water-soluble lignin from Moso bamboo prehydrolyzate. Biotechnology for Biofuels, 2019, 12: 189
25. Bjorkman A. Studies on finely divided wood. Part I. Extraction of lignin with neutral solvents. Svensk Papperstidning, 1956, 59: 477–485
26. Bjorkman A. Lignin and lignin-carbohydrate complexes. Industrial & Engineering Chemistry, 1957, 49: 1395–1398
27. Sluiter J, Sluiter A. Summative mass closure—LAP review and integration: pretreated slurries. NREL/TP-510-48825, 2010
28. Huang C, He J, Narron R, Wang Y, Yong Q. Characterization of kraft lignin fractions obtained by sequential ultrafiltration and their potential application as a biobased component in blends with polyethylene. ACS Sustainable Chemistry & Engineering, 2017, 5: 11770–11779
29. Betts W B, Dart R K, Ball A S, Pedlar S. Biosynthesis and Structure of Lignocellulose. In: Betts W B, ed. Biodegradation: Natural and Synthetic Materials. Berlin: Springer-Verlag, 1991, 139–155
30. Dong H, Zheng L, Yu P, Jiang Q, Wu Y, Huang C, Yin B. Characterization and application of lignin-carbohydrate complexes from lignocellulosic materials as antioxidants for scavenging *in vitro* and *in vivo* reactive oxygen species. ACS Sustainable Chemistry & Engineering, 2019, 8: 256–266
31. Huang C, He J, Du L, Min D, Yong Q. Structural characterization of the lignins from the green and yellow bamboo of bamboo culm (*Phyllostachys pubescens*). Journal of Wood Chemistry and Technology, 2015, 85: 157–172
32. Río J C D, Prinsen P, Cadena E M, Martínez Á T, Gutiérrez A, Rencoret J. Lignin-carbohydrate complexes from sisal (*Agave sisalana*) and abaca (*Musa textilis*): chemical composition and structural modifications during the isolation process. Planta, 2016, 243: 1143–1158
33. Chen X, Li H, Sun S, Cao X, Sun R. Co-production of oligosaccharides and fermentable sugar from wheat straw by hydrothermal pretreatment combined with alkaline ethanol extraction. Industrial Crops and Products, 2018, 111: 78–85
34. Zheng L, Lu G, Pei W, Yan W, Li Y, Zhang L, Huang C, Jiang Q. Understanding the relationship between the structural properties of lignin and their biological activities. International Journal of Biological Macromolecules, 2021, 190: 291–300
35. Gu J, Guo M, Zheng L, Yin X, Zhou L, Fan D, Shi L, Huang C, Ji G. Protective effects of lignin-carbohydrate complexes from wheat stalk against bisphenol a neurotoxicity in zebrafish via oxidative stress. Antioxidants, 2021, 10: 1640
36. Sevastyanova O, Helander M, Chowdhury S, Lange H, Wedin H, Zhang L, Ek M, Kadla J F, Crestini C, Lindström M E. Tailoring the molecular and thermos-mechanical properties of kraft lignin by ultrafiltration. Journal of Applied Polymer Science, 2014, 131: 40799
37. Zhang Y, Wang S, Xu W, Cheng F, Pranovich A, Smeds A, Willför S, Xu C. Valorization of lignin-carbohydrate complexes from hydrolysates of Norway spruce: efficient separation, structural characterization, and antioxidant activity. ACS Sustainable Chemistry & Engineering, 2018, 10: 1447–1456
38. Huang C F, Liu S H, Su C C, Fang K M, Yen C C, Yang C Y, Tang F C, Liu J M, Wu C C, Lee K I, Chen Y W. Roles of ERK/Akt signals in mitochondria-dependent and endoplasmic reticulum stress-triggered neuronal cell apoptosis induced by 4-methyl-2,4-bis(4-hydroxyphenyl)pent-1-ene, a major active metabolite of bisphenol A. Toxicology, 2021, 455: 152764
39. Gu J, Guo M, Yin X, Huang C, Qian L, Zhou L, Wang Z, Wang L, Shi L, Ji G. A systematic comparison of neurotoxicity of bisphenol A and its derivatives in zebrafish. Science of the Total Environment, 2022, 805: 150210
40. Yun J, Wei L, Li W, Gong D, Qin H, Feng X, Li G, Ling Z, Wang P, Yin B. Isolation the high antimicrobial ability lignin from bamboo kraft lignin by organosolv fractionation. Frontiers in Bioengineering and Biotechnology, 2021, 9: 363
41. Santos D K D D N, Barros B R D S, Aguiar L M D S, Filho I J D C, Lorena V M B D, Melo C M L D, Napoleão T H.

Immunostimulatory and antioxidant activities of a lignin isolated from *Conocarpus erectus* leaves. International Journal of Biological Macromolecules, 2020, 150: 169–177

42. Ma Z, Tang J, Li S, Suo E. Reactivity improvement of cellulolytic enzyme lignin via mild hydrothermal modification. Bioorganic Chemistry, 2017, 75: 173–180
43. Wu M, Xu L, Teng C, Xiao X, Hu W, Chen J, Tu W. Involvement of oxidative stress in di-2-ethylhexylphthalate (DEHP)-induced apoptosis of mouse NE-4C neural stem cells. Neurotoxicology, 2019, 70: 41–47
44. Rolas L, Boussif A, Weiss E, Lettéron P, Haddad O, El-Benna J, Rautou P E, Moreau R, Périanin A. NADPH oxidase depletion in neutrophils from patients with cirrhosis and restoration via toll-like receptor 7/8 activation. Gut, 2018, 67: 1505–1516
45. Pan J, Hao X, Yao H, Ge K, Ma L, Ma W. Matrine inhibits mycelia growth of *Botryosphaeria dothidea* by affecting membrane permeability. Journal of Forestry Research, 2019, 30: 1105–1113
46. Li C, Han Y, Hao J, Qin X, Liu C, Fan S. Effects of exogenous spermidine on antioxidants and glyoxalase system of lettuce seedlings under high temperature. Plant Signaling & Behavior, 2020, 15: e182469
47. Rubiolo J A, Mithieux G, Vega F V. Resveratrol protects primary rat hepatocytes against oxidative stress damage: activation of the Nrf2 transcription factor and augmented activities of antioxidant enzymes. European Journal of Pharmacology, 2008, 591: 66–72
48. Yang Q, Pan X. Correlation between lignin physicochemical properties and inhibition to enzymatic hydrolysis of cellulose. Biotechnology and Bioengineering, 2016, 113: 1213–1224
49. Zhang Y, Li H, Jin S, Lu Y, Peng Y, Zhao L, Wang X. Cannabidiol protects against Alzheimer's disease in C. elegans via ROS scavenging activity of its phenolic hydroxyl groups. European Journal of Pharmacology, 2022, 919: 174829
50. Na Y, Woo J, Choi W I, Sung D. Novel carboxylated ferrocene polymer nanocapsule with high reactive oxygen species sensitivity and on-demand drug release for effective cancer therapy. Colloids and Surfaces B: Biointerfaces, 2021, 200: 1115
51. Nenadis N, Samara E, Mantzouridou F T. On the role of the carboxyl group to the protective effect of *o*-dihydroxybenzoic acids to saccharomyces cerevisiae cells upon induced oxidative stress. Antioxidants, 2022, 11(1): 161